

Regional Differences in Elastic Recoil After Percutaneous Transluminal Coronary Angioplasty: A Quantitative Angiographic Study

BENNO J. RENSING, MD, WALTER R. HERMANS, MD, BRADLEY H. STRAUSS, MD,
PATRICK W. SERRUYS, MD, FACC

Rotterdam, The Netherlands

The immediate result of percutaneous transluminal coronary angioplasty is influenced by both plastic and elastic changes of the vessel wall. To evaluate the amount of elastic recoil after coronary balloon angioplasty, the minimal luminal cross-sectional area of the largest balloon used at highest inflation pressure was compared with the minimal luminal vessel cross-sectional area directly after final balloon deflation in 607 lesions (526 patients). Elastic recoil was defined as the difference between balloon cross-sectional area and minimal luminal cross-sectional area of the dilated coronary segment immediately after balloon withdrawal. A videodensitometric analysis technique was used to avoid geometric assumptions on stenosis morphology directly after angioplasty.

Percutaneous transluminal coronary balloon angioplasty remains by far the most applied percutaneous coronary revascularization technique (1). Improvements in guide wire and balloon catheter design allow us to cross and dilate nearly every lesion in the coronary tree, with the exception of some chronically occluded lesions. However, the dilation process itself has not changed basically since the early days of balloon angioplasty and the mechanism by which luminal enlargement is achieved is still the subject of debate (2). Apart from plastic changes (dissection, intimal tear), the immediate result of a balloon angioplasty is also dependent on elastic properties of the vessel wall. We (3) reported earlier that elastic recoil after coronary angioplasty accounted for a nearly 50% decrease in luminal cross-sectional area immediately after balloon deflation. Because the disruptive action of the balloon on the vessel wall causes irregular and asymmetric luminal cross sections (4), cross-sectional area measurements based on automated edge detection techniques are potentially unreliable. Therefore, a videodensitometric analysis technique, which is theoretically independent of geometric assumptions on the shape of the

Mean balloon cross-sectional area was $5.3 \pm 1.6 \text{ mm}^2$ and minimal luminal cross-sectional area after angioplasty was $2.8 \pm 1.4 \text{ mm}^2$. Reference areas before and after angioplasty did not differ (6.0 ± 2.6 and $6.2 \pm 2.6 \text{ mm}^2$, respectively). Univariate analysis revealed that asymmetric lesions, lesions located in less angulated parts of the artery and lesions with a low plaque content showed more elastic recoil. Lesions located in distal parts of the coronary tree were also associated with more elastic recoil probably related to relative balloon oversizing in these distal lesions.

(J Am Coll Cardiol 1991;17:34B-8B)

stenosis, was used. This study was undertaken to determine the amount and the regional distribution of elastic recoil directly after balloon angioplasty with the use of a quantitative angiographic analysis technique.

Methods

Study patients. The study group consisted of 526 patients (607 lesions) who had undergone successful coronary balloon angioplasty, defined as a $<50\%$ diameter stenosis on visual inspection of the postangioplasty angiogram. Patients with stable and unstable angina, as described previously (5), were included; patients with acute myocardial infarction were excluded. The mean age was 56 ± 12 years.

Coronary angioplasty. This was performed by the femoral route with a steerable, movable guide wire system (5). The choice of balloon type (compliant or noncompliant) and manufacturer, inflation pressure and inflation duration were left to the discretion of the operator.

Quantitative Coronary Angiography

Contour detection. All cineangiograms were analyzed using the computer-assisted angiographic analysis system (CAAS), which has previously been described and validated in detail (6,7). To describe briefly the important steps, any area of size $6.9 \times 6.9 \text{ mm}$ (512×512 pixels) in a selected cine frame (overall dimensions $18 \times 24 \text{ mm}$) encompassing the

From the Catheterisation Laboratory, Thoraxcenter, Erasmus University, Rotterdam, The Netherlands. Dr. Strauss is a Research Fellow of the Heart and Stroke Foundation of Canada.

Manuscript received October 19, 1990; accepted November 26, 1990.

Address for reprints: Patrick W. Serruys, MD, Catheterisation Laboratory, Thoraxcenter, Erasmus University, P.O. Box 1738, 3000 DR Rotterdam, The Netherlands.

desired arterial segment can be digitized with a high resolution digital camera. Vessel contours are determined automatically based on the weighted sum of first and second derivative functions applied to the digitized brightness information along scan lines perpendicular to the local centerline directions of an arterial segment. A computer-derived estimation of the original arterial dimension at the site of obstruction is used to define the interpolated reference diameter. The absolute values of the stenosis diameter and the reference diameter are measured by the computer using the known contrast catheter diameter as a scaling device. All contour positions of the catheter and the arterial segment are corrected for pincushion distortion introduced by the image intensifiers. The area between the actual and reconstructed contours at the obstruction site is a measure of the amount of "atherosclerotic plaque" and is expressed in square millimeters. The length of the obstruction is determined from the diameter function on the basis of curvature analysis and expressed in millimeters.

Using the reconstructed borders of the vessel wall, the computer can calculate a symmetry coefficient for the stenosis. Differences in distance between the actual and reconstructed vessel contours on both sides of the lesion are measured. Symmetry is determined by the ratio of these two differences, with the largest distance between actual and reconstructed contours becoming the denominator. Values for symmetry range between 0 for extreme eccentricity to 1 for maximal symmetry (that is, equal distance on both sides between reconstructed and actual contours). The curvature value at the obstruction site, as a measure for coronary bending, is computed as the average value of all the individual curvature values along the centerline of the coronary segment, with the curvature defined by the rate of change of the angle through which the tangent to a curve turns in moving along the curve and which, for a circle, is equal to the reciprocal of the radius.

Densitometric procedure. Constitution of the relation between path length of the X-rays through the artery and the brightness value requires a detailed analysis of the complete X-ray/cine/video chain, including the film development process (8). For the first part of the chain from the X-ray source to the output of the image intensifier, we use Lambert-Beer's law for the X-ray absorption and apply certain models for the X-ray source and the image intensifier. From the output of the image intensifier up to the brightness values in the digital image we use a linear transfer function. Details of this technique have been described elsewhere (9). The cross-sectional area of a vessel is then obtained as follows. The contours of a selected arterial segment are detected, as described before. A profile of brightness values is measured on each scan line perpendicular to the centerline. This profile is transformed into an absorption profile by means of a logarithmic transfer function. The background contribution is estimated by computing the linear regression line through the background points directly to the left and right of the detected contours. Subtraction of this background portion

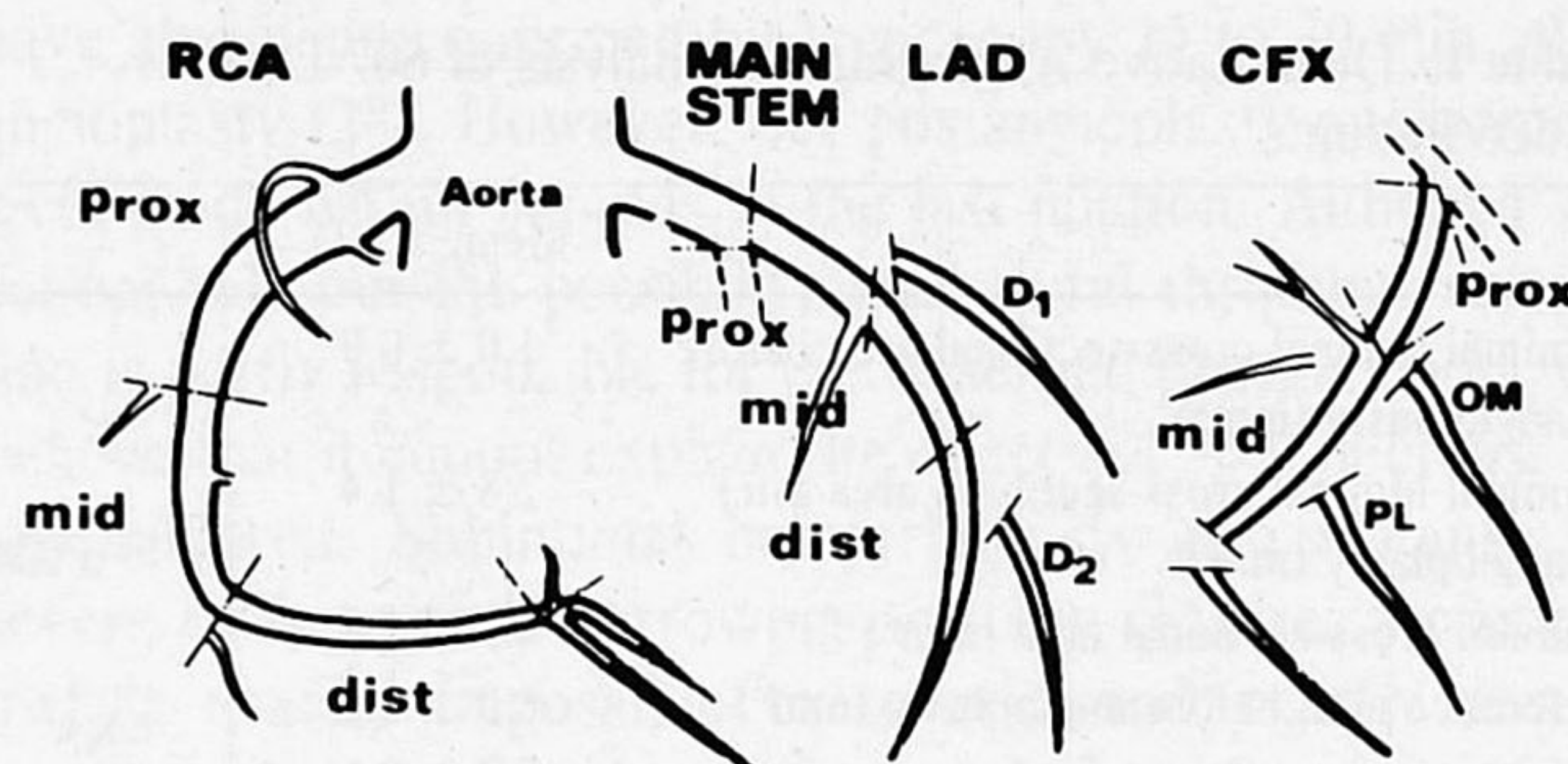


Figure 1. Map with the beginning and end points of the coronary artery segments. CFX = circumflex artery; D₁ and D₂ = first and second diagonal branches, respectively; dist = distal; LAD = left anterior descending artery; mid = mid portion; OM = obtuse marginal branch; PL = posterolateral branch; prox = proximal; RCA = right coronary artery.

yields the net cross-sectional absorption profile. Integration of this function gives a measure for the cross-sectional area at the particular scan line. By repeating this procedure for each scan line, the cross-sectional area function is obtained. Calibration of the densitometric area values is accomplished by comparing the reference area calculated from the diameter measurements (assuming a circular cross section) with the corresponding densitometric area value. The complete procedure has been evaluated with cine films of perspex models of coronary obstructions (8).

Assessment of elastic recoil. Single identical views before and after angioplasty and during complete expansion of the largest balloon at highest inflation pressure were chosen for densitometric analysis. Mean balloon cross-sectional areas were calculated from diameter values, assuming a circular cross section at maximal inflation pressure. The same X-ray setting in terms of kilovoltage and milliamperes was used during the three cine recordings. Vessel segments were analyzed in the least foreshortened projection (that is, perpendicular to the incoming X-ray beam). The same amount of nitrates—either nitroglycerin, 0.1 to 0.3 mg, or isosorbide dinitrate, 1 to 3 mg—was given by intracoronary injection before the pre- and postangioplasty cine recordings. These agents were administered to maximally dilate the vessel and, hence, to control the varying influence of vasomotor tone on luminal dimensions. Elastic recoil was then calculated as the difference between the minimal luminal cross-sectional area after angioplasty and the mean balloon cross-sectional area (mm²). The time between final balloon deflation and the postangioplasty cine recordings was usually <1 min. To compare the amount of recoil in different parts of the coronary tree, absolute values were normalized for reference area at the obstruction site. The beginning and end points of the major coronary segments are shown in Figure 1. The definitions are slightly modified from those of the American Heart Association (10).

Statistical analysis. The individual quantitative data were used to calculate mean values and SD. Univariate analysis of variance was performed for the continuous variables. A

Table 1. Quantitative Angiographic Analysis of 607 Lesions in 526 Patients

	Mean \pm SD	
Minimal luminal cross-sectional area before angioplasty (mm ²)	1.0 \pm 0.9	
Minimal luminal cross-sectional area after angioplasty (mm ²)	2.8 \pm 1.4] p < 0.0001
Balloon cross-sectional area (mm ²)	5.3 \pm 1.6	
Reference area before angioplasty (mm ²)	6.0 \pm 2.6] NS
Reference area after angioplasty (mm ²)	6.2 \pm 2.6	
Elastic recoil (mm ²)	2.5 \pm 1.4	
Lesion length (mm)	6.5 \pm 2.7	
Symmetry value	0.5 \pm 0.3	
Plaque area (mm ²)	7.2 \pm 4.4	
Curvature value (U)	17.5 \pm 10.5	

probability value < 0.05 was considered significant. To avoid arbitrary subdivision of data, cutoff criteria for continuous variables were derived by dividing the data into three groups so that each group contained about one third of the population. The group with the highest amount of recoil was then compared with the two other groups (11). This method of subdivision is consistent for all variables and thus avoids any bias in selection of subgroups that might be undertaken to emphasize a particular point.

Results

Angiographic lesion characteristics. The mean minimal luminal cross-sectional area predilation and postdilation and the balloon cross-sectional area for the 607 lesions are shown in Table 1. The mean minimal luminal cross-sectional area was 1.0 \pm 0.9 mm² before and 2.8 \pm 1.4 mm² after angioplasty. The mean balloon cross-sectional area was 5.3 \pm 1.6 mm². The mean amount of elastic recoil was 2.5 \pm 1.4 mm². These data indicate a nearly 50% loss of maximally achievable cross-sectional area directly after balloon deflation. Reference area before angioplasty was not changed significantly by angioplasty. Other quantitative angiographic lesion characteristics of the 607 lesions are shown in Table 1. Table 2 shows the grouping of the quantitative data for statistical analysis (based on the tertiles), the numbers in each group and the amount of recoil relative to vessel size. Asymmetric lesions, lesions with a small plaque area and

Table 2. Quantitative Angiographic Variables and Elastic Recoil in 607 Coronary Lesions

	Yes (recoil/reference)	No (recoil/reference)	p Value
Lesion length <5.1 mm	200 (0.49)	407 (0.44)	NS
Symmetry <0.37	205 (0.50)	402 (0.43)	p < 0.05
Plaque area <4.7 mm ²	199 (0.55)	408 (0.41)	p < 0.01
Curvature <12.5 U	206 (0.51)	401 (0.40)	p < 0.01

Values indicate number of lesions and recoil normalized for reference diameter (recoil/reference).

Table 3. Regional Distribution of Elastic Recoil in 607 Coronary Lesions

	N	Recoil/ Reference Ratio		Balloon/ Artery Ratio	
LAD prox	118	0.43] p < 0.01	0.90] p < 0.01
LAD mid	120	0.48		0.97	
LAD dist	23	0.61		1.20	
LCx prox	39	0.41] p < 0.01	0.80] p < 0.01
LCx mid	54	0.41		0.90	
Obtuse marginal	29	0.47		0.93	
Posterolateral	24	0.54] p < 0.01	1.10] p < 0.01
RCA prox	71	0.28		0.78	
RCA mid	76	0.38		0.98	
RCA dist	50	0.40		0.98	

dist = distal; LAD = left anterior descending artery; LCx = circumflex artery; mid = mid portion; prox = proximal; RCA = right coronary artery.

lesions located in straighter arterial segments (low curvature value) were associated with significantly more elastic recoil.

Regional distribution of elastic recoil. Data on elastic recoil in the different parts of the coronary tree are summarized in Table 3. Data on diagonal branches and the ramus descendens posterior in left dominant systems are omitted because of the small number of segments dilated in this series (5 and 0, respectively). Recoil, normalized for vessel size, increased from proximal to distal parts for all three major coronary branches. This increase in elastic recoil corresponds to a significant increase in the balloon/artery ratio from proximal to distal parts of the coronary arteries.

Discussion

Mechanisms of lesion dilation in balloon angioplasty. Dotter and Judkins (12) in 1964 envisioned that balloon angioplasty worked by remodeling and compression of the atheroma because initial pathologic studies revealed little intimal destruction and no evidence of dissection. However, the vast majority of atherosclerotic plaques in human coronary arteries are composed of incompressible, dense fibrocollagenous tissue and therefore it appears unlikely that plaque compression plays a major role in balloon angioplasty. However Kaltenbach et al. (13) observed in an in vitro model a reduction in weight and thickness of the atherosclerotic vessel wall after pressure application. This reduction was more pronounced in lipoidotic plaques, suggesting that fluid expression from atherosclerotic tissue could play some role in the luminal widening achieved by angioplasty (13). According to Sanborn et al. (14), part of the angioplasty mechanism consists of stretching the vessel wall with a resulting fusiform dilation or localized aneurysm formation. If the lesion is eccentric, then the least diseased portion of the vessel wall will stretch (15).

Castaneda-Zuniga et al. (16) found that angioplasty induced paralysis by overstretching the vessel wall beyond its limits of elasticity and suggested this to be the cause of

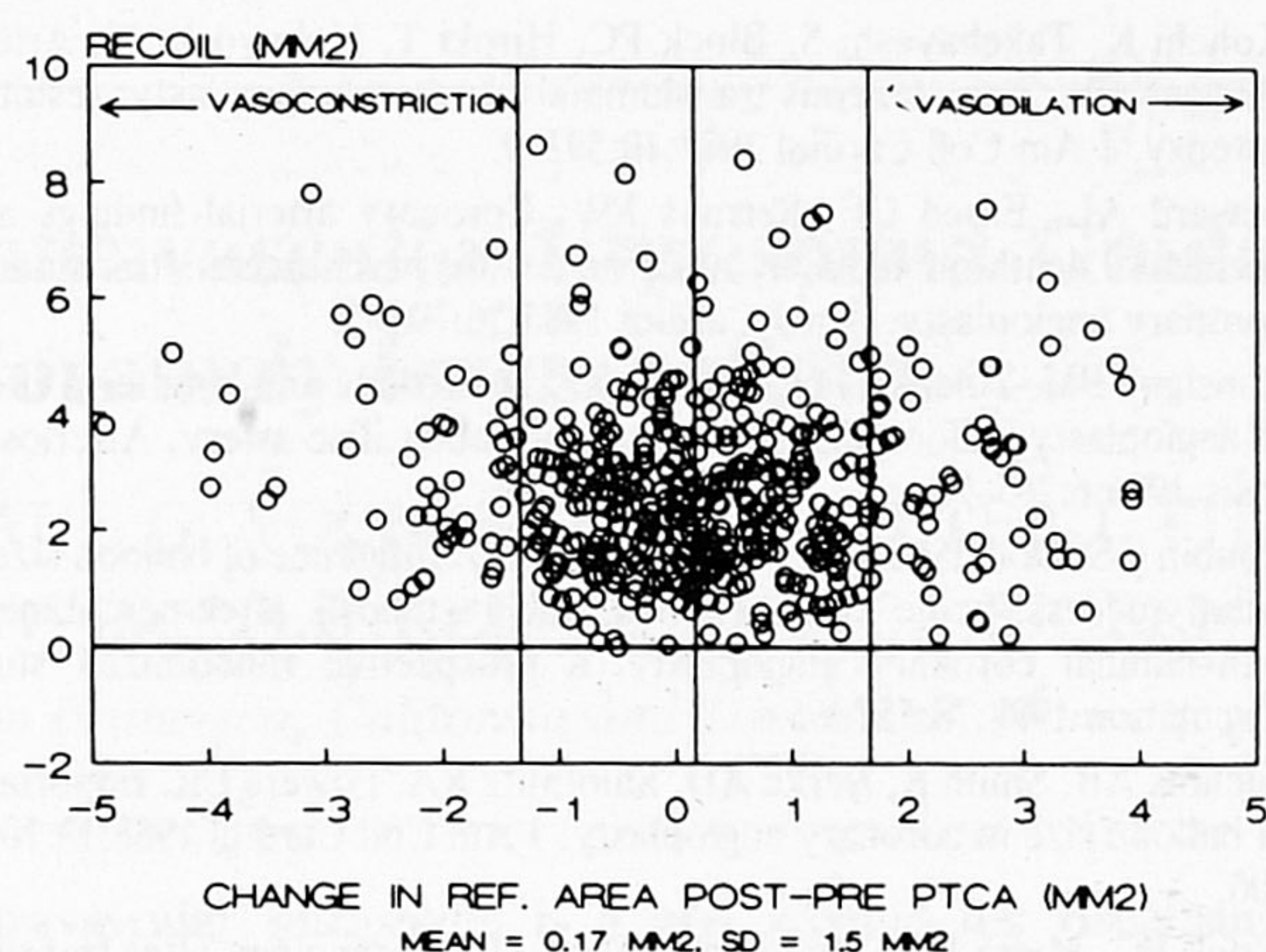


Figure 2. Is vasomotion part of the recoil phenomenon? Scatter plot of the difference in reference area after angioplasty from that before angioplasty (POST-PRE PTCA) against the amount of recoil for each of the 607 lesions (see text for explanation).

permanent luminal widening after balloon angioplasty. This widening was associated with histopathologic features of smooth muscle cell lysis and twisted nuclei. These correlates of severe medial damage were not found in human arteries examined post mortem after recent dilation (17,18). In *in vitro* models of balloon angioplasty in rabbit iliac artery, rabbit aorta and pig carotid artery, only severe oversizing of the balloon produced impairment of vasoconstrictor responsiveness (19). Because it is becoming clear that oversizing of the balloon leads to an increased complication rate (20) and that satisfactory initial results can be obtained by conservative balloon sizing (20,21), deliberate oversizing of the angioplasty balloon is not common in our institution. This is reflected by the mean balloon/artery ratio of 0.95 in our study. Thus, arterial paralysis must be questioned as an explanation for the luminal widening achieved by angioplasty in human coronary arteries. The most consistent finding after angioplasty is disruption and splitting of the neointima and localized intimal dissection (22).

Mechanisms of early restenosis. Early lesion recurrence after balloon angioplasty is most likely due to vasoconstriction, intimal flaps, mural thrombus formation or subintimal hemorrhage (23-27). Fischell et al. (26) showed that vasoconstriction after balloon angioplasty could be rapidly reversed by intracoronary injection of nitrates. Because we gave intracoronary nitrates before the pre- and postangioplasty cine recordings, it seems unlikely that the amount of recoil observed was caused by vasomotion. In Figure 2 the difference between the postangioplasty and preangioplasty reference area is plotted against the amount of recoil for each site. The values are randomly distributed around the mean value of 0.17 mm², suggesting the absence of vasoconstriction at the postangioplasty cine recording.

Despite full heparinization, platelet deposition and the formation of a nonocclusive mural thrombus are not uncommon findings in postmortem hearts obtained from patients who die in the first hours after angioplasty (27). Such findings

have also been confirmed by angiography 15 to 30 min after angioplasty (28). However, our postangioplasty angiograms were made within minutes of the last dilation. Although we cannot rule out the possibility that mural thrombus formation is partly responsible for the observed phenomenon, we believe that it cannot explain the observed 50% decrease in luminal area. Subintimal hemorrhage is also a cause of severe early luminal narrowing or acute closure, a process that is usually impossible to reverse and nearly always results in failed angioplasty. In this study only successfully dilated lesions were analyzed.

Factors leading to elastic recoil. Eccentric lesions showed significantly more elastic recoil. This can be explained by the fact that in such lesions, a part of the vessel circumference is not diseased. The portion that is not diseased will be preferentially stretched by the balloon with subsequently more elastic recoil (15). Lesions with a high bending and a large bulk of atherosclerotic plaque showed less elastic recoil. It is known that dissections are more common in this type of lesion (24,29). The gross disruption of the vessel wall and the atherosclerotic plaque associated with an angiographically visible dissection might release the cicatrizing effect of the plaque that had chronically affected the media. Release of this force may allow the media to return to its more normal outer diameter and thus reduce some of the recoil effect.

Recoil relative to vessel size increases from proximal to distal parts of the coronary arteries. This phenomenon is due to the tendency of balloon oversizing in distal parts of the coronary tree (Table 3). If a vessel is stretched within its limits of elasticity, it will return toward its rest state along an elastic hysteresis loop. More stretch should thus give more elastic recoil. It is difficult to discern whether the oversizing is based on economic grounds (an extra balloon for a second distal site nearly doubles the cost of angioplasty disposable equipment) or is due to visual overestimation of smaller caliber vessels. In our series, a minority of 40 patients underwent multilesion dilation including a proximal and a distal segment. In 31 of these cases, the same balloon was used for the proximal and distal stenoses. Mean balloon cross-sectional area was 4.7 ± 1.2 mm² for the proximal stenosis and 4.6 ± 1.2 mm² for the distal stenosis ($p = \text{NS}$). Reference area was 5.8 ± 2.4 mm² for the proximal lesions and 4.6 ± 2.2 mm² for the distal lesions ($p < 0.01$). Balloon artery ratio was 0.85 ± 0.5 for these proximal lesions and 1.0 ± 0.5 for distal lesions ($p < 0.01$).

References

1. Bourassa MG, Alderman EL, Bertrand M, et al. Report of the joint ISFC/WHO task force on coronary angioplasty. *Circulation* 1988;78:780-9.
2. Waller BF. "Crackers, breakers, stretchers, drillers, scrapers, shavers, burners, welders and melters"—the future treatment of atherosclerotic coronary artery disease?: a clinical-morphologic assessment. *J Am Coll Cardiol* 1989;13:969-87.
3. Rensing BJ, Hermans WRM, Beatt KJ, et al. Quantitative angiographic

- assessment of elastic recoil after percutaneous transluminal coronary angioplasty. *Am J Cardiol* 1990;66:1039-44.
4. Serruys PW, Reiber JH, Wijns W, et al. Assessment of percutaneous transluminal coronary angioplasty by quantitative coronary angiography: diameter versus densitometric area measurements. *Am J Cardiol* 1984;54:482-8.
 5. de Feyter PJ, Serruys PW, van den Brand M, et al. Emergency coronary angioplasty in refractory unstable angina. *N Engl J Med* 1985;313:342-6.
 6. Reiber JHC, Kooijman CJ, Slager CJ, et al. Coronary artery dimensions from cineangiograms: methodology and validation of a computer-assisted analysis procedure. *IEEE Trans Med Imaging* 1984;M13:131-41.
 7. Reiber JH, Serruys PW, Kooijman CJ, et al. Assessment of short-, medium-, and long-term variations in arterial dimensions from computer-assisted quantitation of coronary cineangiograms. *Circulation* 1985;71:280-8.
 8. Reiber JHC, Serruys PW, Slager CJ. Quantitative Coronary and Left Ventricular Cineangiography: Methodology and Clinical Application. Dordrecht, The Netherlands: Martinus Nijhoff, 1986:165-8.
 9. Reiber JHC, Slager CJ, Schuurbiens JCH, et al. Transfer functions of the X-ray cine video chain applied to digital processing of coronary cineangiograms. In: Heintzen PH, Brennecke R, eds. *Digital Imaging in Cardiovascular Radiology*. Stuttgart-New York: Georg Thieme Verlag, 1983:89-104.
 10. Austen WG, Edwards JE, Frye RL, et al. A reporting system in patients evaluated for grading of coronary artery disease. Report of the Ad Hoc Committee for Grading Coronary Artery Disease, Council on Cardiovascular Surgery, American Heart Association. *Circulation* 1975;51:7-40.
 11. Rothman KJ. *Modern Epidemiology*. Boston: Little, Brown, 1986:115-25.
 12. Dotter CT, Judkins MP. Transluminal treatment of atherosclerotic obstructions: description of new technique and a preliminary report of its application. *Circulation* 1964;30:654-70.
 13. Kaltenbach M, Beyer J, Walter S, Klepzig H, Schmidts L. Prolonged application of pressure in transluminal coronary angioplasty. *Cathet Cardiovasc Diagn* 1984;10:213-9.
 14. Sanborn TA, Faxon DP, Haudenschild CG, Gottsman SB, Ryan TJ. The mechanism of transluminal angioplasty: evidence for aneurysm formation in experimental atherosclerosis. *Circulation* 1983;68:1136-40.
 15. Waller BF. Coronary luminal shape and the arc of disease-free wall: morphologic observations and clinical relevance. *J Am Coll Cardiol* 1985;6:1100-1.
 16. Castaneda-Zuniga WR, Formanek A, Tadavarthy M, et al. The mechanism of balloon angioplasty. *Radiology* 1980;135:565-71.
 17. Kohchi K, Takebayashi S, Block PC, Hiroki T, Nobuyoshi M. Arterial changes after percutaneous transluminal coronary angioplasty: results at autopsy. *J Am Coll Cardiol* 1987;10:592-9.
 18. Soward AL, Essed CE, Serruys PW. Coronary arterial findings after accidental death immediately after successful percutaneous transluminal coronary angioplasty. *Am J Cardiol* 1985;56:794-5.
 19. Consigny PM, Tulenko TN, Nicosia RF. Immediate and long-term effects of angioplasty-balloon dilation on normal rabbit iliac artery. *Arteriosclerosis* 1986;6:265-76.
 20. Roubin GS, Douglas JS Jr, King SB III, et al. Influence of balloon size on initial success, acute complications, and restenosis after percutaneous transluminal coronary angioplasty: a prospective randomized study. *Circulation* 1988;78:557-65.
 21. Nichols AB, Smith R, Berke AD, Shlofmitz RA, Powers ER. Importance of balloon size in coronary angioplasty. *J Am Coll Cardiol* 1988;13:1094-100.
 22. Block PC, Myler RK, Sterzer S, Fallon JT. Morphology after transluminal angioplasty in human beings. *N Engl J Med* 1981;305:382-5.
 23. Cowley MJ, Dorros G, Kelsey SF, Van Raden M, Detre KM. Emergency coronary bypass surgery after coronary angioplasty: the National Heart, Lung, and Blood Institute's Percutaneous Transluminal Coronary Angioplasty Registry experience. *Am J Cardiol* 1984;53:22C-6C.
 24. Ellis SG, Roubin GS, King SB III, et al. Angiographic and clinical predictors of acute closure after native vessel coronary angioplasty. *Circulation* 1988;77:372-9.
 25. Simpfendorfer C, Belardi J, Bellamy G, Galan K, Franco I, Hollman Y. Frequency, management and follow-up of patients with acute coronary occlusions after percutaneous transluminal coronary angioplasty. *Am J Cardiol* 1987;59:267-9.
 26. Fischell TA, Derby G, Tse TM, Stadius ML. Coronary artery vasoconstriction routinely occurs after percutaneous transluminal coronary angioplasty: a quantitative arteriographic analysis. *Circulation* 1988;78:1323-34.
 27. Waller BF, Gorfinkel HJ, Rogers FJ, Kent KM, Roberts WC. Early and late morphologic changes in major epicardial coronary arteries after percutaneous transluminal coronary angioplasty. *Am J Cardiol* 1984;53:42C-7C.
 28. Uchida Y, Hasegawa K, Kawamura K, Shibuya I. Angioscopic observation of the coronary luminal changes induced by percutaneous transluminal coronary angioplasty. *Am Heart J* 1989;117:769-76.
 29. Zollkofer C, Chain J, Salomonowitz E, et al. Percutaneous transluminal angioplasty of the aorta. *Radiology* 1983;151:355-63.